J. Fluid Mech. (2011), *vol.* 668, *pp.* 351–362. © Cambridge University Press 2011
doi:10.1017/S0022112010005793

A stochastic view of isotropic turbulence decay

MARCELLO MELDI[1]†, PIERRE SAGAUT[2] AND DIDIER LUCOR[2]

[1]DIMeC Dipartimento di Ingegneria Meccanica e Civile, Università degli studi di Modena e Reggio Emilia, 41100 Modena, Italy

[2]Institut Jean Le Rond d'Alembert, UMR 7190, 4 Place Jussieu, Case 162, Université Pierre et Marie Curie, Paris 6, F-75252 Paris CEDEX 5, France

(Received 21 May 2010; revised 25 October 2010; accepted 3 November 2010)

A stochastic eddy-damped quasi-normal Markovian (EDQNM) approach is used to investigate self-similar decaying isotropic turbulence at a high Reynolds number ($400 \leqslant Re_\lambda \leqslant 10^4$). The realistic energy spectrum functional form recently proposed by Meyers & Menevau (*Phys. Fluids*, vol. 20, 2008, p. 065109) is generalized by considering some of the model constants as random parameters, since they escape measure in most experimental set-ups. The induced uncertainty on the solution is investigated, building response surfaces for decay power-law exponents of usual physical quantities. Large-scale uncertainties are considered, the emphasis being put on Saffman and Batchelor turbulences. The sensitivity of the solution to initial spectrum uncertainties is quantified through probability density functions of the decay exponents. It is observed that the initial spectrum shape at very large scales governs the long-time evolution, even at a high Reynolds number, a parameter which is not explicitly taken into account in many theoretical works. Therefore, a universal asymptotic behaviour in which kinetic energy decays as t^{-1} is not detected. However, this decay law is observed at finite Reynolds numbers with low probability for some initial conditions.

Key words: generalized polynomial chaos, isotropic turbulence

1. Introduction

The decay of isotropic turbulence is one of the oldest topics considered in the field of turbulence theory, which started with the seminal studies of Taylor (1935). Comprehensive reviews are presented by Batchelor (1953), Hinze (1975), Monin & Yaglom (1975), Davidson (2004) and Sagaut & Cambon (2008). One of the most famous related issues deals with the existence and uniqueness of self-similar regimes, in which global turbulent quantities, such as turbulence kinetic energy q, behave like

$$q(x) = A\,(x/M_u - x_0/M_u)^n \quad \text{or} \quad q(t) = A'\,(t - t_0)^n\,, \tag{1.1}$$

where x, x_0, M_u, A, A' and n are the distance downstream the grid, the virtual origin of isotropic turbulence, the mesh size of the grid used to trigger turbulence, two parameters and the decay exponent, respectively. Equivalence between space- and time-dependent decay is recovered thanks to Taylor's frozen turbulence hypothesis.

† Email address for correspondence: marcellomeldi@gmail.com

https://doi.org/10.1017/S0022112010005793 Published online by Cambridge University Press

Influential works of Kolmogorov (1941), Batchelor & Proudman (1956) and Saffman (1967*a*) have shown that the value of the decay exponent n (or equivalent power-law exponent for other global physical quantities) is not unique but mainly governed by initial conditions (see also Lavoie, Djenedi & Antonia 2007; Uberoi 1963). The theory of self-similar decay has been addressed by many authors, among them George (1992) and Speziale & Bernard (1992), in which an explicit dependency with respect to initial conditions is taken into account. More specifically, the shape of the spectrum at very large scales is observed to be of primary importance. In fact, several spectrum shapes at very large scales are known to be physically realizable in isotropic turbulence. This point has been discussed by many authors, since it is related to the famous controversy dealing with existence of invariants in high-Reynolds-number decaying turbulence. Saffman (1967*a*) showed that the invariance of the Birkhoff–Saffman invariant $L = \int \langle \boldsymbol{u} \cdot \boldsymbol{u}' \rangle \, \mathrm{d}\boldsymbol{r}$ during turbulence decay is related to linear momentum conservation. The associated kinetic energy spectrum behaves like $E(k \to 0) = Lk^2/4\pi^2$ and theoretical analysis shows that the turbulent kinetic energy decays as $q(t) \sim t^{-6/5}$. If $L = 0$, the resulting condition is referred to as the Batchelor turbulence: the corresponding large scales behave like $E(k \to 0) = Ik^4/24\pi^2$, where $I = \int \boldsymbol{r}^2 \langle \boldsymbol{u} \cdot \boldsymbol{u}' \rangle \, \mathrm{d}\boldsymbol{r}$ is the Loitsyansky integral. In this case, the turbulent kinetic energy scales as $q(t) \sim t^{-10/7}$.

The Reynolds number is also known to be a key parameter. In fact, low-Reynolds-number flows, which are mostly driven by viscous linear effects, do not exhibit the same power-law exponent as high-Reynolds-number flows (see e.g. Batchelor & Townsend 1948; Burattini *et al.* 2006).

The prediction of power-law exponent starting from a simplified kinetic energy spectrum shape was introduced by Comte-Bellot & Corrsin (1966), who considered a two-range spectrum and dimensional analysis. This method was then revised by Saffman (1967*a*,*b*). Following these works, the spectrum is divided into two power-law ranges joining at a peak located at k_L: one for the very large scales, $E(k \leqslant k_L) = Ak^{\sigma}, \sigma \in [1, 4]$, and a Kolmogorov-type inertial range at smaller scales, $E(k \geqslant k_L) = C_K \varepsilon^{2/3} k^{-5/3}$, where σ, C_K and ε denote the spectrum slope at large scales, the Kolmogorov constant and the turbulent dissipation rate, respectively. While Saffman ($\sigma = 2$) and Batchelor ($\sigma = 4$) turbulences have been extensively analysed, other possibilities have also been considered, e.g. $\sigma = 1$ and $\sigma = 3$ in Clark & Zemach (1998) and Oberlack (2002). Predictions dealing with power-law exponents of some usual physical quantities obtained using the two-range spectrum model in the high-Reynolds-number case are presented in the first column of table 1. This analysis was then further developed to investigate the sensitivity of the power-law exponent to additional features of the initial condition. Skrbrek & Stalp (2000) considered a smoothed form of the spectrum at k_L, along with internal intermittency, clipping in the dissipation range and large-scale saturation effects. An important conclusion is that saturation induced by boundary condition yields a dramatic change in the power-law exponent, making it very difficult to distinguish between a saturated high-Reynolds-number regime and a free low-Reynolds-number evolution. The truncation of energy spectrum at very large scales also corrupts the computation of integral quantities, such as integral length scale (Wang & George 2002). The use of two power-law ranges was also shown to be inconsistent with the existence of a helicity-based invariant in the limit of infinitely high Reynolds numbers, a three-range model being necessary to this end; see Frenkel & Levich (1983) and Frenkel (1984).

An important point is that experimental validation of theoretically predicted behaviour is elusive for many reasons. First, it is almost impossible to enforce

https://doi.org/10.1017/S0022112010005793 Published online by Cambridge University Press

Quantity	CBC formula	$\sigma=1$	$\sigma=2$	$\sigma=3$	$\sigma=4$
q	$-2\dfrac{\sigma+1}{\sigma+3}$	−1.005 (<1 %)	−1.213 (1.2 %)	−1.342 (<1 %)	−1.4014 (2 %)
L	$\dfrac{2}{\sigma+3}$	0.457 (8 %)	0.402 (<1 %)	0.336 (1.8 %)	0.307 (7.8 %)
η	$\dfrac{3\sigma+5}{4(\sigma+3)}$	0.502 (1 %)	0.556 (1.2 %)	0.588 (<1 %)	0.603 (<1 %)
λ	$1/2$	0.501 (<1 %)	0.505 (1 %)	0.505 (1 %)	0.505 (1 %)
ε	$\dfrac{-3\sigma-5}{\sigma+3}$	−2.009 (<1 %)	−2.226 (1.2 %)	−2.352 (<1 %)	−2.412 (<1 %)
Re_λ	$\dfrac{1-\sigma}{2(\sigma+3)}$	−0.0006	−0.1006 (<1 %)	−0.166 (<1 %)	−0.195 (8.9 %)
Re_L	$\dfrac{1-\sigma}{\sigma+3}$	−0.044	−0.204 (2.3 %)	−0.335 (<1 %)	−0.393 (8.3 %)

TABLE 1. Power-law exponents in the high-Reynolds-number isotropic turbulence decay. Comte-Bellot–Corrsin (CBC) formula denotes expressions obtained via dimensional analysis. Other columns display values computed using classical deterministic EDQNM simulations, using a two-range CBC spectrum at initial time and ($Re_\lambda(t=0)=10^4$). Relative errors with respect to the theoretical predictions are reported between parentheses. The quantities are: q, turbulent kinetic energy; L, integral length scale; η, Kolmogorov length scale; λ, Taylor microscale; ε, turbulent dissipation rate; $Re_\lambda=\sqrt{2q/3}\lambda/\nu$; $Re_L=\sqrt{2q/3}L/\nu$.

the spectrum shape at very large scales in laboratory experiments. Second, in most cases, the large-scale spectrum shape is not directly measured but deduced from the measured decay law and theoretical relations which bridge between them. Third, identification of the three free parameters in (1.1), namely A (or A'), x_0 and n, leads to the definition of a non-robust optimisation problem, which introduces a significant uncertainty in the experimental estimates as discussed by Mohamed & LaRue (1990) and Krogstad & Davidson (2010). Finally, it has been recently shown that spurious saturation effects may occur in numerical simulations due to the use of periodic boundary conditions, and that very large computational domains must be used in order to preclude such problem (Ishida Davidson & Kaneda 2006). Looking at open literature, it appears that large enough domains have not been used in most published papers, precluding definitive analysis. Another important issue is the possible existence of a universal decay regime, in which kinetic energy should decay as t^{-1}. Such a regime is predicted by some theoretical models such as George (1992) and Speziale & Bernard (1992), but it has not been observed up to now and seems at least partially contradictory with a strong dependency upon initial conditions.

The aim of the present paper is to further investigate the sensitivity of the power-law exponents with respect to details of the initial kinetic energy spectrum. To this end, the spectrum shape function very recently introduced by Meyers & Menevau (2008) is considered. This model, which accounts for both intermittency and bottleneck effects, includes several intrinsic parameters, which escape measurement in laboratory experiments. Therefore, they must be considered as epistemic uncertainties and modelled as random variables. A direct consequence of dependency with respect to initial conditions is that a stochastic approach must be used instead of the usual deterministic one, and that power-law exponents must be characterized using numerical tools streaming from probability theory. In the present paper, the response

https://doi.org/10.1017/S0022112010005793 Published online by Cambridge University Press

surfaces of power-law exponents of several quantities of interest (kinetic energy q, integral scale L, Kolmogorov scale η) are constructed as a polynomial approximation obtained from a stochastic spectral projection method (Ko, Lucor & Sagaut 2008). Samples are generated using a high-fidelity model whose accuracy has been assessed for isotropic turbulence decay, namely the EDQNM model (Orszag 1970; Sagaut & Cambon 2008). The EDQNM solver makes it possible to account for fine details of the kinetic energy spectrum.

This paper is structured as follows. The turbulent energy spectrum model used in the present study is presented in § 2, along with the response-surface building strategy, which is based on the polynomial chaos representation (Ghanem & Spanos 1991). High-Reynolds decay with uncertain spectrum shape at large scales is investigated. In § 3, the spectrum slope parameter σ itself is considered as a random parameter, in order to mimic experimental uncertainties. Then, the influence of other large-scale parameters for both Saffman and Batchelor turbulences is further analysed in § 4.

2. Energy spectrum model and response-surface parametrization

The determination of the turbulent energy spectrum shape is an old but still very active research topic. Many models have been proposed (see for instance Hinze 1975; Monin & Yaglom 1975), varying in complexity and approaches, spanning from simple definitions to more accurate models with the drawback of introducing a significant number of free parameters. In the present work, the energy spectrum model proposed by Meyers & Menevau (2008) is used, since it accounts for all known features of the kinetic energy spectrum. A convenient approach is to express them as functionals of random variables. It is written as follows:

$$E(k) = C_K \varepsilon^{2/3} k^{-5/3} (kL)^{-\beta} f_L(kL) f_\eta(k\eta), \tag{2.1}$$

where β is the intermittency correction in the inertial range of the spectrum. It is taken equal to $\beta = \mu/9$, with $\mu = 0.25$ being the value commonly found in the literature. Following Meyers & Menevau (2008), the Kolmogorov constant C_K is taken equal to 2.0173, $L = E_t^{3/2}/\varepsilon$ is the integral length scale, and η is the Kolmogorov length scale. The functions f_L and f_η shape the spectrum at very large and very small scales, respectively. These are expressed as

$$f_L(kL) = \left(\frac{kL}{[(kL)^p + \alpha_5]^{1/p}} \right)^{5/3+\beta+\sigma}, \quad f_\eta(k\eta) = \mathrm{e}^{-\alpha_1 k\eta} B(k\eta). \tag{2.2}$$

The bottleneck correction $B(k\eta)$ is

$$B(k\eta) = 1 + \frac{\alpha_2 (k\eta/\alpha_4)^{\alpha_3}}{1 + (k\eta/\alpha_4)^{\alpha_3}}. \tag{2.3}$$

The two shape functions introduce five arbitrary parameters. Parameters α_1–α_4 govern the shape of the spectrum at high wavenumbers, while α_5 controls it at low wavenumbers. In Meyers & Menevau (2008), it is proposed to compute these parameters by solving a system of five equations, which are related to the recovery of target values for the turbulent kinetic energy, the turbulent dissipation (or equivalently the enstrophy), the palinstrophy (or equivalently the longitudinal velocity derivative skewness) and constraints derived considering some possible universal feature of the dissipation spectrum.

In § 3, large-scale uncertainty is modelled considering σ, p and α_5 as independent random variables with a *uniform* distribution, the range of variation being adjusted based on open literature. The choice of uniform distributions means that we do not

https://doi.org/10.1017/S0022112010005793 Published online by Cambridge University Press

favour any particular parametric values within the ranges of interest. Coefficients α_1–α_4 are estimated using the procedure proposed by Meyers & Menevau (2008) for each realization, enforcing the same global quantities (enstrophy, palinstrophy, position and value of the compensated dissipation spectrum peak) at the initial time. Large-scale dependency of Batchelor and Saffman turbulences is further analysed by fixing σ and considering p, α_5 and μ as uncertain parameters. The response surface of the solution with respect to uncertain random variables is built in the present work using the generalized polynomial chaos (gPC) method, which is a non-statistical method used to solve stochastic differential and stochastic partial differential equations. This method was recently applied in the field of turbulence research by Lucor, Meyers & Sagaut (2007). Following this approach, the power-law decay exponent of each physical quantity under consideration, which is now a random variable depending nonlinearly on the uncertain parameters, can be represented thanks to the following polynomial expansion with pseudo-spectral accuracy:

$$n(\boldsymbol{\xi}) = \sum_{l=0}^{\infty} n_l \Phi_l(\boldsymbol{\xi}), \tag{2.4}$$

where Φ_l is an orthogonal polynomial set with respect to the joint probability density function (p.d.f.) of the random array $\boldsymbol{\xi}$, whose components are the independent random variables used to model the parametric uncertainty. In practical cases, the expansion is truncated and the expansion coefficients n_l are computed using a Galerkin-type projection method, relying on a multidimensional Gaussian quadrature. In the present work, all random variables were assumed to follow a uniform distribution, leading to the use of Legendre polynomials. It was checked that in all cases, the use of third-order polynomials along with four quadrature points (per dimension) yields fully converged results. Note that a deterministic EDQNM simulation is performed at each quadrature point, leading to 4^N simulations, where N is the number of uncertain parameters under consideration. For each quadrature point in the uncertainty space, an energy spectrum fitting relations (2.1)–(2.3) is set as an initial condition, a self-similar regime with the same time-independent spectrum shape coefficients and decay exponent is obtained via the EDQNM simulation and then the corresponding power-law coefficients are measured. The gPC method is then applied as a post-processing tool, reconstructing the response surface of the power-law coefficients over the continuous uncertainty space starting from the discrete values computed at the quadrature points. The EDQNM deterministic solver was validated taking a simplified two-range Comte-Bellot–Corrsin (CBC) spectrum as the initial condition for $\sigma = 1, 2, 3$ and 4 at a high Reynolds number ($Re_\lambda(t=0) = 10^4$). The results were very close to those recovered using simple dimensional-analysis-based calculations (see table 1). Discrepancies observed in the case $\sigma = 4$ stem from the fact that, in the Batchelor turbulence, EDQNM predicts the existence of a time drift of the coefficient A in $L(t) = A(t - t_0)^n$, which is not distinguished from the power-law behaviour. An important point is that $\lambda \sim t^{1/2}$ is recovered within 1 % error on the exponent in all cases.

3. High-Reynolds-number turbulence decay with an uncertain large-scale spectrum shape

Uncertainty about the large-scale kinetic energy distribution at a high Reynolds number is investigated first, considering σ, p and α_5 as random variables with a *uniform* distribution. Details are displayed in table 2. Note that this case is typically

https://doi.org/10.1017/S0022112010005793 Published online by Cambridge University Press

Spectrum parameter	Mean value	Range	Reported variations
σ	2.5	[1, 4]	$[1, 4] \cup [+\infty]$
p	1.5	[1, 2]	[1.5, 2]
α_5	4.1	[3.9, 4.3]	[3.967, 4.224]
μ	0.25	[0.2, 0.3]	[0.2, 0.3]

TABLE 2. Uncertain parameters of the kinetic energy spectrum, modelled as *uniform* random variables. Mean value and range are related to present simulations, while reported variations refer to the variability reported in open literature.

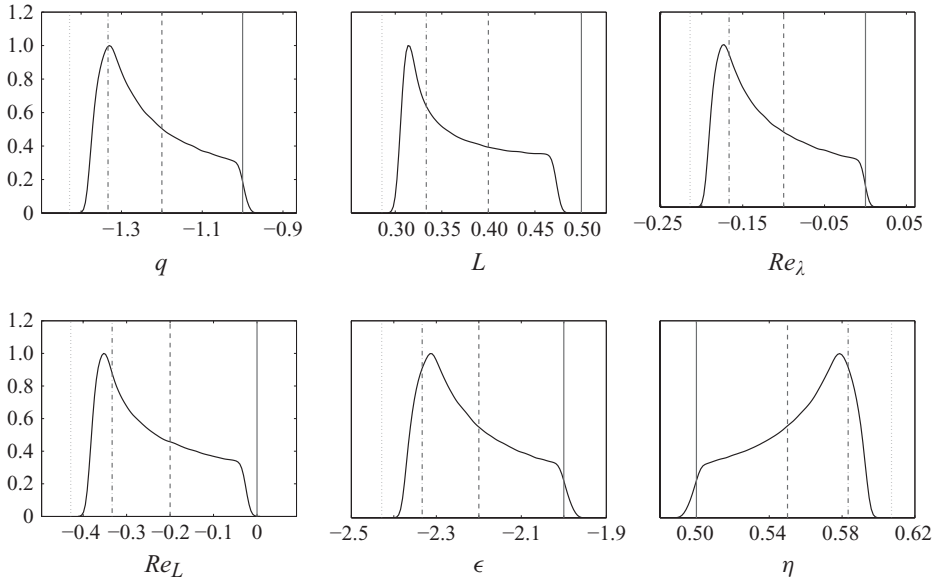


FIGURE 1. P.d.f.s of power-law exponents. Vertical lines refer to theoretical values retrieved from the CBC analysis. Solid line, $\sigma = 1$; dashed line, $\sigma = 2$ (Saffman turbulence); dash-dotted line, $\sigma = 3$; dotted line, $\sigma = 4$ (Batchelor turbulence).

representative of laboratory experiments in which the large-scale spectrum is neither controlled nor known. In order to be sure that self-similar states are reached, which corresponds to high-Reynolds-number dynamics, the initial Reynolds number is set equal to $Re_\lambda(t=0) = 10^4$. With this value, $Re_\lambda(t) > 400$ is obtained during the self-similar evolution of the system. Statistical results are displayed in table 3 and figure 1, which show parameters and p.d.f.s of the power-law exponent for several global quantities, as computed from gPC/EDQNM-based response surfaces. A very significant variability is observed on all exponents, which is mainly due to the large-scale exponent σ, as predicted by theoretical analysis. In the present case, the use of Sobol's coefficients (Sobol 1993) shows that this parameter is responsible for 97 %–99 % of the total variance, indicating that at high Reynolds number, σ has a leading impact over the turbulence decay, as already known by the seminal work of Batchelor & Townsend (1948). The exponent p, which governs the smoothness of the energy spectrum peak, is observed to be the second leading parameter. It

https://doi.org/10.1017/S0022112010005793 Published online by Cambridge University Press

https://doi.org/10.1017/S0022112010005793 Published online by Cambridge University Press

Exponent	n_d	$\bar{n}$	c_v	$[n_{min}, n_{max}]$	Q_{95}	n_p	ς_σ	ς_p	ς_{α_5}
q	−1.242	−1.227	8.6 %	[−1.384, −0.980]	−1.030	−1.330	9.85×10^{-1}	1.40×10^{-2}	3.73×10^{-6}
L	0.363	0.374	13.4 %	[0.304, 0.475]	0.462	0.314	9.99×10^{-1}	9.46×10^{-4}	1.93×10^{-6}
Re_λ	−0.128	−0.118	45.6 %	[−0.194, 0]	−0.018	−0.173	9.92×10^{-1}	7.05×10^{-3}	1.18×10^{-6}
Re_L	−0.258	−0.240	42.9 %	[−0.388, −0.017]	−0.054	−0.353	9.94×10^{-1}	5.69×10^{-3}	1.63×10^{-7}
ε	−2.227	−2.218	4.7 %	[−2.380, −1.968]	−2.025	−2.315	9.76×10^{-1}	2.36×10^{-2}	8.09×10^{-6}
η	0.557	0.554	4.7 %	[0.492, 0.595]	0.588	0.579	9.76×10^{-1}	2.36×10^{-2}	8.09×10^{-6}

TABLE 3. Statistical data related to power-law exponents. The terms n_d, $\bar{n}$, c_v, n_{min}, n_{max}, Q_{95}, n_p and ς refer to the deterministic value associated with the mean value of the uncertain parameters, statistical mean value, coefficient of variation (standard deviation referred to as $\bar{n}$), minimum value, maximum value, 95 % quantile value, most probable value (i.e. peak of the p.d.f.) and the normalized partial variance associated with the subscript variable, respectively.

is observed that the maximum variability (with c_v close to 45 %) is obtained for Reynolds number exponents, because of the combination of uncertainties on kinetic energy and the characteristic length scale under consideration, rendering the use of these parameters very complex in laboratory experiments. Another important point is that most probable values n_p, which can be interpreted as the exponent values mostly to be observed in uncontrolled realizations of decaying turbulence, differ significantly from deterministic values, n_d, and the mean values computed from the response surface, $\bar{n}$. The two latter values are seen to be quite close to each other, showing that n_d may be substituted into $\bar{n}$ as a relevant surrogate for faster analysis.

Comparisons with data from the literature are mostly restricted to the kinetic energy exponent, since other physical quantities have been much less documented. A significant variability has been reported in experimental works: Comte-Bellot & Corrsin (1966) reported $-1.3 < n < -1.15$, while Warhaft & Lumley (1978) found $n \sim -1.34$. Hot-wire measurements by Lavoie *et al.* (2007) are in the range $-1.22 \pm 0.02 < n < -1.04 \pm 0.02$. Antonia *et al.* (2003) reported $n \sim -1.25$. Lower values such as $n \sim -1$ can be found, e.g. Batchelor & Townsend (1948). The present range of variation $[n_{min}, n_{max}]$ is in very good agreement with values reported by Mohamed & LaRue (1990) (e.g. figure 13 therein). This is also true looking at the predicted most probable value $n_p \simeq -1.33$. Lower values reported recently in Krogstad & Davidson (2010), i.e. $n = -1, 13 \pm 0.02$, are also encompassed by the present variation range. The lowest predicted value is -1.384, indicating that a lower value may be due to low Reynolds number and/or finite domain size effects. The same satisfactory agreement is found for other quantities. Antonia *et al.* (2003) reported $n \sim -0.125$ for Re_λ, $n \sim 0.36$–0.40 for L.

Looking at figure 1 one observes that for all physical quantities, the p.d.f. does not encompass the theoretical value associated with Batchelor turbulence ($\sigma = 4$). This is also coherent with results displayed in table 3. In fact, this is related to the existence of a time drift of the prefactor in that case, and to previous observations reported by many authors, who observed a violation of the hypothesis of permanence of large eddies. Exponent values associated with $\sigma = 1$ have a very low probability, indicating that this case is very difficult to identify using real-life experiments. Interestingly, most probable exponent values are close to those of $\sigma = 3$. An important conclusion here is that it is very difficult to derive the distribution kinetic energy at large scales using power-law exponents of global quantities, and that direct measurement of the spectrum is the only safe way to obtain conclusive results on that point.

4. Stochastic analysis of Saffman and Batchelor turbulences

We now consider uncertainty for fixed deterministic σ values, analysing the two canonical cases known as Saffman turbulence ($\sigma = 2$) and Batchelor turbulence ($\sigma = 4$). The stochastic approach is developed considering the set of parameters p, α_5 and μ as *uniform* random variables (see table 2). The results, reported in table 4, comply with the corresponding conservation laws and in the case of Saffman turbulence the theoretical relation correlating n_ε and n_L is recovered with an error lower than 2 %. The stochastic analysis of low-order moments (e.g. coefficient of variation c_v) indicates that small variances are recovered for both cases, up to 4 % for the Reynolds number. A sensitivity analysis indicates that initial conditions depend almost exclusively on p. However, extreme events (e.g. maximum and minimum power-law exponents) are instead quite distant from one another, spanning from

https://doi.org/10.1017/S0022112010005793 Published online by Cambridge University Press

	n_d	$\bar{n}$	c_v	$[n_{min}, n_{max}]$	Q_{95}	n_p
			Saffman turbulence ($\sigma = 2$)			
q	−1.188	−1.185	1 %	[−1.200, −1.158]	−1.163	−1.199
L	0.397	0.398	0.2 %	[0.397, 0.400]	0.400	0.397
Re_λ	−0.097	−0.096	4.2 %	[−0.101, −0.087]	−0.088	−0.101
Re_L	−0.196	−0.195	3.3 %	[−0.203, −0.179]	−0.182	−0.202
ε	−2.181	−2.177	0.7 %	[−2.199, −2.144]	−2.149	−2.195
η	0.545	0.544	0.7 %	[0.536, 0.550]	0.549	0.549
			Batchelor turbulence ($\sigma = 4$)			
q	−1.370	−1.365	1.4 %	[−1.388, −1.317]	−1.326	−1.385
L	0.305	0.307	0.9 %	[0.304, 0.315]	0.313	0.304
Re_λ	−0.189	−0.187	3.8 %	[−0.195, −0.169]	−0.173	−0.194
Re_L	−0.380	−0.376	3.3 %	[−0.390, −0.344]	−0.350	−0.388
ε	−2.362	−2.355	1 %	[−2.385, −2.295]	−2.307	−2.381
η	0.590	0.589	1 %	[0.574, 0.596]	0.596	0.595

TABLE 4. Statistical data related to power-law exponents, in the case of large-scale uncertainty at fixed values of σ. For details, see the caption to table 3.

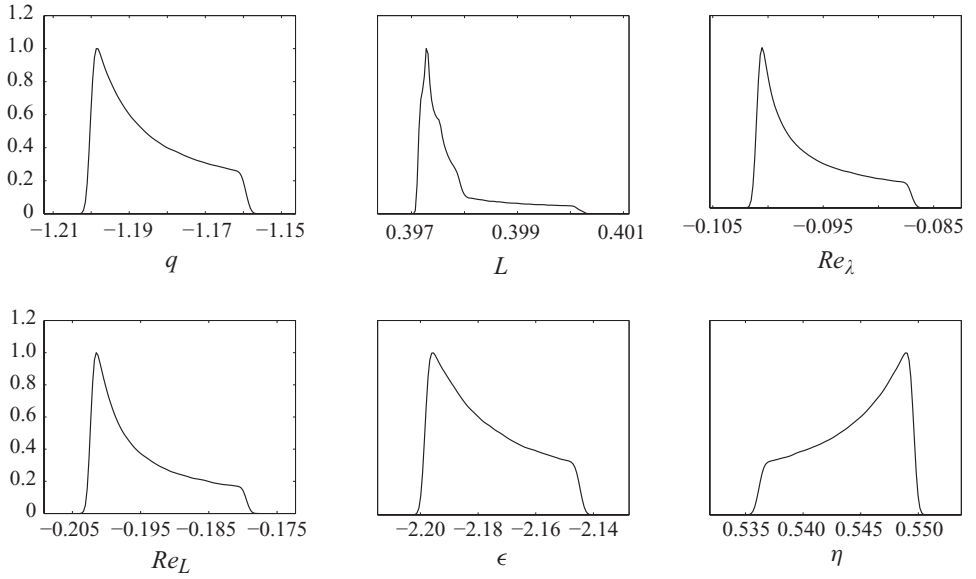


FIGURE 2. The p.d.f. of power-law exponents for the Saffman turbulence ($\sigma = 2$) for $Re_\lambda(t) > 400$.

values close to the theoretical ones to values even 10 %–15 % lower in magnitude. The same trend is noticeable in the p.d.f. reported in figures 2 and 3, where the most probable value is always quite close to the theoretical value. The introduction of uncertainties over the model constant of the energy spectrum functional form leads to a high probability of recovering a turbulence decay state whose characteristics are close to the theoretical value, but the probability of a significant gap is not negligible. In particular, when the width of the inertial range is reduced (wide and smooth spectrum peak for small values of p), the turbulence decay is characterized by a lower

https://doi.org/10.1017/S0022112010005793 Published online by Cambridge University Press

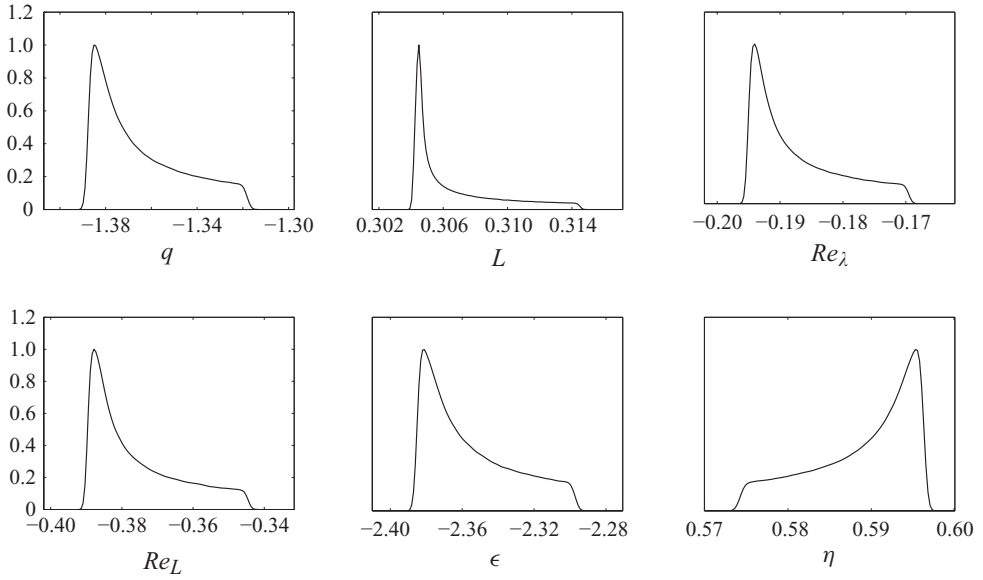


FIGURE 3. The p.d.f. of power-law exponents for the Batchelor turbulence ($\sigma = 4$) for $Re_\lambda(t) > 400$.

magnitude of the power-law coefficients. On the contrary, at high p values, i.e. if the energy spectrum shape is similar to the CBC spectrum model, power-law exponents get closer to the theoretical exponents. An important remark is that ranges of variation of n do not overlap. Therefore, tentative values of σ can be deduced from n in the high-Reynolds-number, unbounded isotropic turbulence inverting CBC formula (see table 1). Note that $n \sim -1.3$ should be associated with Batchelor turbulence, while $-1.2 \leqslant n \leqslant -1.15$ may indicate the occurrence of Saffman-type turbulence.

5. Concluding remarks

The present results, based on the EDQNM closure for the Lin equation and not on the sole dimensional analysis, confirm that the slope of the spectrum at large scales at initial time is the leading parameter that governs the decay regime. A $q \sim t^{-1}$ decay can be observed at finite time and finite Reynolds numbers for $\sigma \simeq 1$, a small variability with other large-scale parameters being observed. In that regime, turbulence decays at almost constant Re_λ. The occurrence of this regime shows that $n = -1$ is not tied to the existence of a universal asymptotic regime, and that experimental evidence of the existence of such a universal regime may be very difficult to obtain, unless σ is accurately and independently measured. The dependency upon σ is observed to remain, even at Reynolds numbers considered in the present study ($Re_\lambda > 400$), which are higher than those considered in almost all existing published results. The variability observed for Batchelor and Saffman turbulences with respect to details of spectrum shape is relatively small, leading to an almost univoque identification of σ from n, inverting relations retrieved from the CBC theory, at least at a high Reynolds number and restricting the analysis to integer values for σ. Present results show no evidence of the existence of a universal regime with $q \sim t^{-1}$ at high but *finite* Reynolds numbers, even looking at long-time evolution. Another point is that even though isotropy is perfectly satisfied and finite size effects are absent (the

https://doi.org/10.1017/S0022112010005793 Published online by Cambridge University Press

ratio-integral length scale/lowest resolved scale is greater than 250), the decay exponent is governed by σ. Therefore, convergence towards a single value reported in some experimental works when isotropy is refined (e.g. Lavoie *et al.* 2007) might be the signature of the large-scale spectrum produced by a given experimental set-up rather than a true universal value.

REFERENCES

Antonia, R. A., Smalley, R. J., Zhou, T., Anselmet, F. & Danaila, L. 2003 Similarity of energy structure functions in decaying homogeneous isotropic turbulence. *J. Fluid Mech.* **487**, 245–269.

Batchelor, G. K. 1953 *The Theory of Homogeneous Turbulence*. Cambridge University Press.

Batchelor, G. K. & Proudman, I. 1965 The large-scale structure of homogeneous turbulence. *Phil. Trans. R. Soc. Lond.* A **248**, 369–405.

Batchelor, G. K. & Townsend, A. A. 1948 Decay of turbulence in the final period. *Proc. R. Soc. Lond.* A **194**, 527–543.

Burattini, P., Lavoie, P., Agrawal, A., Djenidi, L. & Antonia, R. A. 2006 Power law of decaying homogeneous isotropic turbulence at low Reynolds number. *Phys. Rev.* E **73**, 066304.

Clark, T. T. & Zemach, C. 1998 Symmetries and the approach to statistical equilibrium in isotropic turbulence. *Phys. Fluids* **10** (11), 2846–2858.

Comte-Bellot, G. & Corrsin, S. 1966 The use of a contraction to improve the isotropy of grid-generated turbulence. *J. Fluid Mech.* **25**, 657–682.

Davidson, P. A. 2004 *Turbulence: An Introduction for Scientists and Engineers.* Oxford University Press.

Frenkel, A. L. 1984 Decay of homogeneous turbulence in three-range models. *Phys. Lett.* A **102** (7), 298–302.

Frenkel, A. L. & Levich, E. 1983 Statistical helicity invariant and decay of inertial turbulence. *Phys. Lett.* A **98** (1–2), 25–27.

Hinze, J. O. 1975 *Turbulence.* McGraw-Hill Series in Mechanical Engineering.

George, W. K. 1992 The decay of homogeneous isotropic turbulence. *Phys. Fluids* A **4** (7), 1492–1509.

Ghanem, R. G. & Spanos, P. 1991 *Stochastic Finite Elements: A Spectral Approach.* Springer.

Ishida, T., Davidson, P. A. & Kaneda, Y. 2006 On the decay of isotropic turbulence. *J. Fluid Mech.* **564**, 455–475.

Ko, J., Lucor, D. & P. Sagaut, P. 2008 Sensitivity of two-dimensional spatially developing mixing layers with respect to uncertain inflow conditions. *Phys. Fluids* **20** (7), 077102–077120.

Kolmogorov, A. N. 1941 On the degeneration of isotropic turbulence in an incompressible viscous fluid. *Dokl. Akad. Nauk. SSSR* **31** (6), 538–541.

Krogstad, P.-Å. & Davidson, P. A. 2010 Is grid turbulence Saffman turbulence? *J. Fluid Mech.* **642**, 373–394.

Lavoie, P., Djenedi, L. & Antonia, R. A. 2007 Effects of initial conditions in decaying turbulence generated by passive grids. *J. Fluid Mech.* **585**, 395–420.

Lucor, D., Meyers, J. & Sagaut, P. 2007 Sensitivity analysis of large-eddy simulations to subgrid-scale-model parametric uncertainty using polynomial chaos. *J. Fluid Mech.* **585**, 255–279.

Meyers, J. & Menevau, C. 2008 A functional form for the energy spectrum parametrizing bottleneck and intermittency effects. *Phys. Fluids* **20** (6), 065109.

Mohamed, M. S. & LaRue, J. C. 1990 The decay power law in grid-generated turbulence. *J. Fluid Mech.* **219**, 195–214.

Monin, A. S. & Yaglom, A. M. 1975 *Statistical Fluid Mechanics: Mechanics of Turbulence,* vol. 2. MIT Press.

Oberlack, M. 2002 On the decay exponent of isotropic turbulence. *Proc. Appl. Math. Mech.* **1** (1), 294–297.

Orszag, S. A. 1970 Analytical theories of turbulence. *J. Fluid Mech.* **41**, 363–386.

Saffman, P. J. 1967*a* The large-scale structure of homogeneous turbulence. *J. Fluid Mech.* **27**, 581–593.

https://doi.org/10.1017/S0022112010005793 Published online by Cambridge University Press

Saffman, P. J. 1967*b* A note on decay of homogeneous turbulence. *Phys. Fluids* **10**, 1349–1352.

Sagaut, P. & Cambon, C. 2008 *Homogenous Turbulence Dynamics*. Cambridge University Press.

Skrbrek, L. & Stalp, S. R. 2000 On the decay of homogeneous isotropic turbulence. *Phys. Fluids* **12** (8), 1997–2019.

Sobol, I. 1993 Sensitivity estimates for nonlinear mathematical models. *Math. Modeling Comput. Exp.* **1**, 407–414.

Speziale, C. G. & Bernard, P. S. 1992 The energy decay in self-preserving isotropic turbulence revisited. *J. Fluid Mech.* **241**, 645–667.

Taylor, G. I. 1935 Statistical theory of turbulence. *Proc. R. Soc. Lond.* A **151**, 421–444.

Uberoi, M. S. 1963 Energy transfer in isotropic turbulence. *Phys. Fluids* **6** (8), 1048–1056.

Wang, H. & George, W. K. 2002 The integral scale in homogeneous isotropic turbulence. *J. Fluid Mech.* **459**, 429–443.

Warhaft, Z. & Lumley, J. L. 1978 An experimental study of the decay of temperature fluctuations in grid-generated turbulence. *J. Fluid Mech.* **88**, 659–684.

https://doi.org/10.1017/S0022112010005793 Published online by Cambridge University Press